Electronic Supplementary Information (ESI)

2D → 3D polycatenated Zn(II) metal-organic framework with good chemical stability as the fluorescent sensor toward salicylaldehyde, acetylacetone and $H_2PO_4^-$

Ya-Ping Li,[a]* Jian-Hua Zhang,[a] Xiao-Xia Zhang[a] and Sui-Jun Liu[b]*

[a]School of Chemistry and Chemical Engineering, Shanxi University, Taiyuan 030006, P.R. China. E-mail: yapingli2007@163.com (Y.-P. Li)

[b]School of Chemistry and Chemical Engineering, Jiangxi Provincial Key Laboratory of Functional Molecular Materials Chemistry, Jiangxi University of Science and Technology, Ganzhou 341000, Jiangxi Province, P.R. China. E-mail: sjliu@jxust.edu.cn (S.-J. Liu)

Section 1. Experiments

Synthesis of BBIP

The synthetic route of BBIP is shown in Scheme S1. A mixture of 3,5-dibromopyridine (2.37 g, 10 mmol), benzimidazole (3.54 g, 30 mmol), 1,10-phenanthroline (0.90 g, 5 mmol) and K_2CO_3 (9.95 g, 72 mmol) in the presence of CuI (0.46 g, 2.4 mmol) as a catalyst was dissolved in 125 mL DMF with a 250 mL flask and refluxed under a N_2 atmosphere for 72 h. After being cooled down to room temperature, 40 mL of distilled water was added to facilitate the workup. The mixture was extracted three times with CH_2Cl_2 (120 mL), then the organic phase was further washed with distilled water and dried with anhydrous $MgSO_4$. After the filtration and evaporation, the yellow crude was obtained. Finally, colorless strip crystals of 3,5-bis(1*H*-benzo[d]imidazol-1-yl)pyridine (BBIP) were obtained by recrystallization of the yellow crude in the mixed solvent of CH_2Cl_2 and CH_3OH with a yield of 50%. ^{1}H NMR (600 MHz, $CDCl_3$): 9.01 (s, 2H), 8.28 (s, 2H), 8.14 (s, 1H), 7.95-7.96 (t, J = 6 Hz, 5 Hz, 2H), 7.62-7.63 (m, 2H), 7.44 (dd, J = 8.9, 5.0 Hz, 4H).

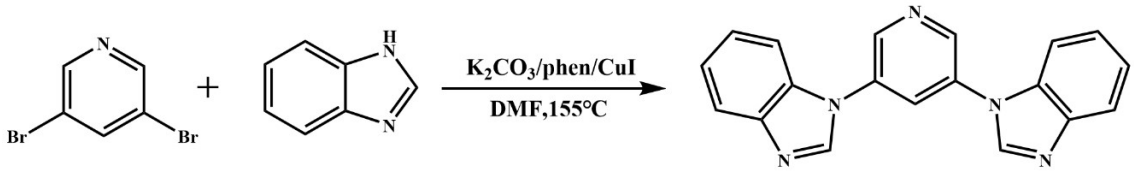

Scheme S1. The synthetic route of BBIP

Section 2. General Characterizations

Table S1. Selected bond lengths (Å) and angles (°) for **JXUST-44**[a]

Zn1—N1^{i}	2.045(5)	Zn1—N3	2.046(5)
Zn1—O5	1.979(12)	Zn1—O1	1.948(12)
N1^{i}—Zn1—N3	97.42(18)	O5—Zn1—N1^{i}	110.7(4)
O5—Zn1—N3	127.1(4)	O1—Zn1—N1^{i}	103.3(4)
O1—Zn1—N3	107.4(4)	O1—Zn1—O5	108.2(5)

[a]Symmetry code: (i) x+1, y, z.

Table S2. SHAPE analysis of the Zn^{II} ion in **JXUST-44**.

ions	label	shape	symmetry	Distortion (τ)
Zn1	SP-4	Square	D_{4h}	29.001
	T-4	**Tetrahedron**	$\boldsymbol{T_d}$	**0.949**
	SS-4	Seesaw	C_{2v}	5.533
	vTBPY-4	Vacant trigonal bipyramid	C_{3v}	2.688

Table S3. Comparison of the sensitivity of **JXUST-44** with previously reported luminescent sensors toward SA and acac.

Analytes	Materials	type	LOD	Reference
SA	CDB-Am	turn-on effect	0.94 μM	S1
	$\{[(CH_3)_2NH_2]_{0.7}[Tb_2(BTDBA)_{1.5}(lac)_{0.7}$-$(H_2O)_2]\cdot solvents\}_n$ (**JXUST-19**)	turn-on effect	0.19 ppm	S2
	$[Cd(BIBT)(3,4\text{-}TDC)]_n$ (**JXUST-27**)	turn-off effect	0.087 μM	S3
	$\{[Cd(BBIP)(TBIP)]\cdot EtOH\}_n$	turn-off effect	0.42 ppm	S4
	$\{[(CH_3)_2NH_2][Eu(TCPB)(H_2O)_2]\cdot DMF\}_n$	turn-off effect	0.095 ppm	S5
	$[Zn(BBIP)(2,6\text{-}NDC)]_n$	turn-off effect	0.074 ppm	**This work**
acac	$\{[Cd(HL)(bpy)]\cdot 1.25H_2O\cdot 1.5DMF\}_n$ (**LCU-107**)	turn-on effect	0.136 ppm	S6
	$\{[(CH_3)_2NH_2]_5[Tb_5(TBAPy)_5]\cdot solvent\}_n$	turn-on effect	0.129 ppm	S7
	$\{[Zn_2(oxdz)_2(tpbn)]\cdot 14H_2O\}_n$	turn-on effect	4 ppm	S8
	$[Ni(L)(NPTA)\cdot H_2O]_n$	turn-off effect	0.79 μM	S9
	$[Cd_2(L2)_2(DCTP)_2]_n$	turn-off effect	0.636 μM	S10
	$[Zn(BBIP)(2,6\text{-}NDC)]_n$	turn-on effect	0.103 mM	**This work**

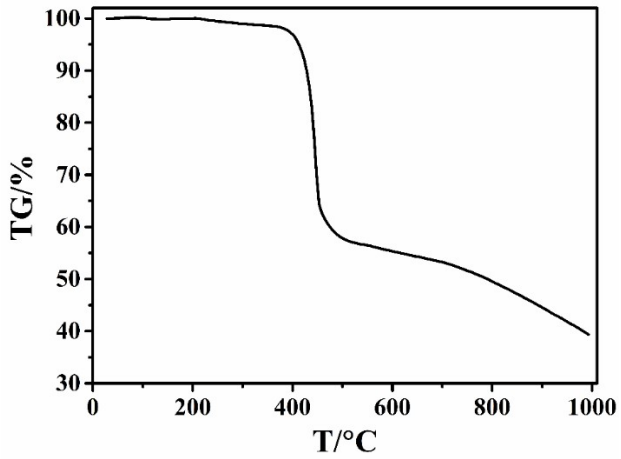

Fig. S1 The TG curve for **JXUST-44**.

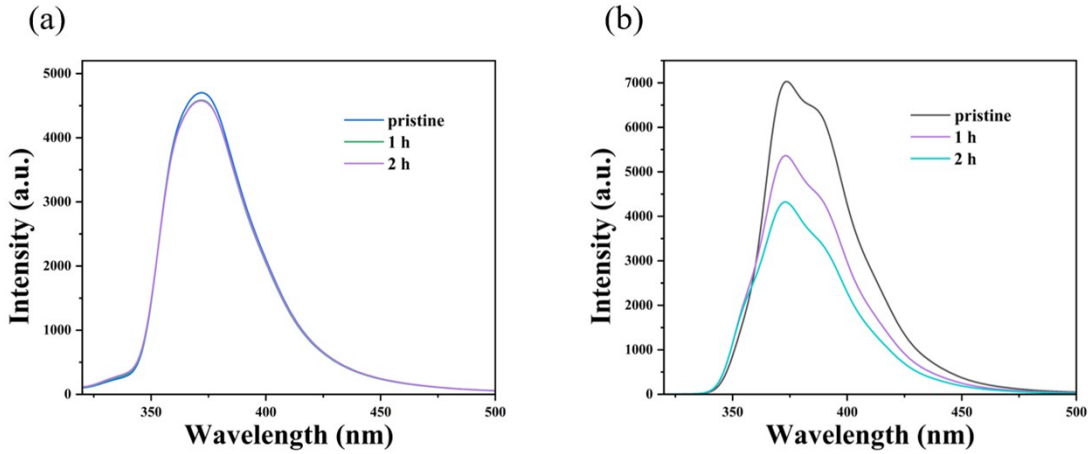

Fig. S2 Fluorescence stability of **JXUST-44** after soaking in (a) DMF and (b) water for 2 hours.

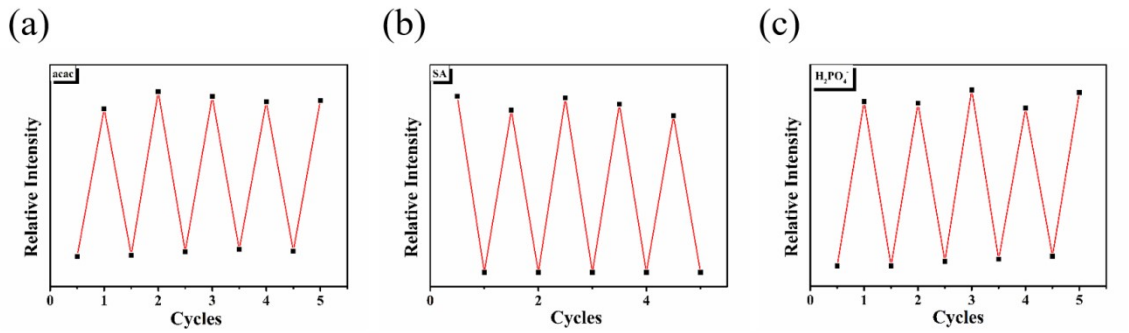

Fig. S3 Relative fluorescent intensity of **JXUST-44** in five cycles of the sensing experiments toward (a) acac, (b) SA and (c) $H_2PO_4^-$.

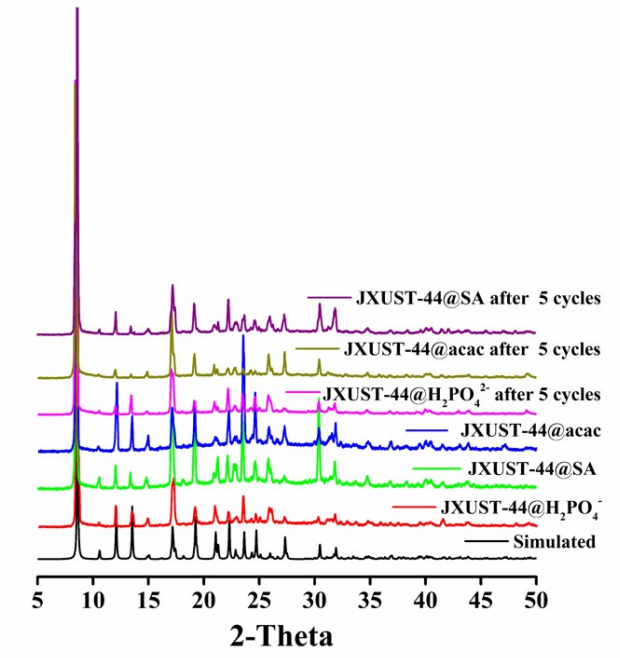

Fig. S4 The PXRD patterns of **JXUST-44** soaked in DMF solution containing acac/SA/$H_2PO_4^-$ for 24 h and acac/SA/$H_2PO_4^-$ sensing for five times.

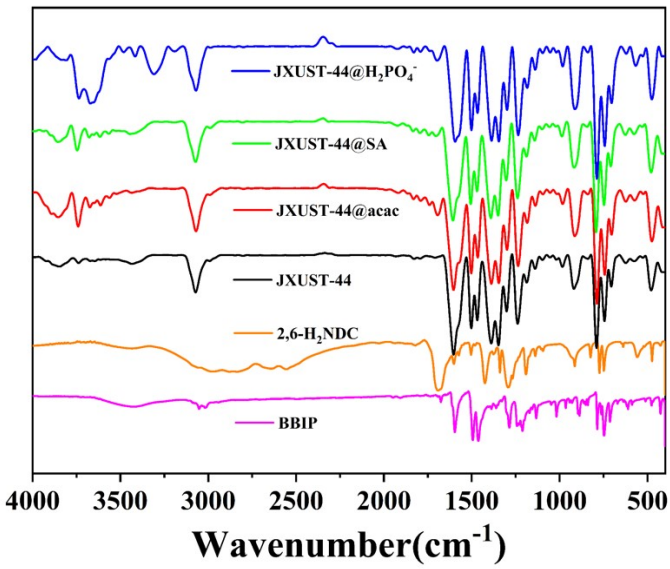

Fig. S5 The IR spectra of BBIP, 2,6-H_2NDC, **JXUST-44**, **JXUST-44**@acac, **JXUST-44**@SA and **JXUST-44**@$H_2PO_4^-$.

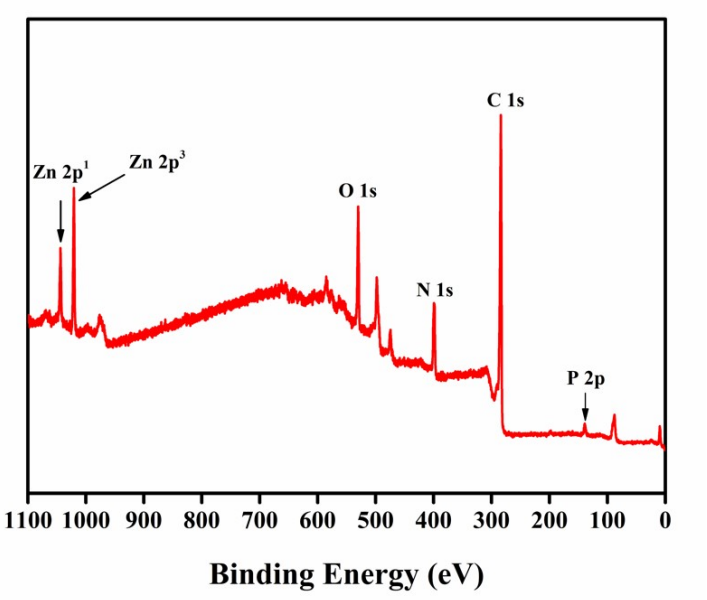

Fig. S6 The XPS of **JXUST-44** after soaked in DMF solution containing $H_2PO_4^-$.

References

S1 S. B. Chen, S. N. Zheng, S. J. Jiang, H. Y. Guo and F. F. Yang, *Anal Bioanal. Chem.*, 2021, **413**, 1955–1966.

S2 K. Wang, T. F. Zheng, J. L. Chen, H. R. Wen, S. J. Liu and T. L. Hu, *Inorg. Chem.*, 2022, **61**, 16177–16184.

S3 X. L. Yan, X. Q. Cao, C. R. Deng, T. F. Zheng, S. L. Yao and S. J. Liu, *CrystEngComm*, 2023, **25**, 2366–2371

S4 L. H. Wu, S. L. Yao, J. Li, H. Xu, T. F. Zheng, S. J. Liu, J. L. Chen and H. R. Wen, *CrystEngComm*, 2021, **23**, 482–491.

S5 B. C. Chen, C. Q. Xiao, J. J. Hu, Y. Peng, H. R. Wen and S. J. Liu, *Inorg. Chem.,* 2023, **62**, 6255–6262.

S6 Y. E. Yu, Y. H. Wang, H. J. Xu, J. Lu, H. W. Wang, D. C. Li, J. M. Dou, Y. W. Li and S. N. Wang, *CrystEngComm,* 2020, **22**, 3759–3767.

S7 Y. G. Li, J. J. Hu, J. L. Zhang, S. J. Liu, Y. Peng and H. R. Wen, *CrystEngComm*, 2022, **24**, 2464–2471.

S8 A. Gogia and S. K. Mandal, *ACS Appl. Mater. Interfaces*, 2022, **14**, 16357–16368.

S9 H. Zhu, C. Han, Y. H. Li and G. H. Cui, *J. Solid State Chem.*, 2020, **282**, 121132.

S10 Y. S. Shi, D. Liu, L. S. Fu, Y. H. Li and G. Y. Dong, *CrystEngComm*, 2020, **22**, 4079–4093.